American Mineralogist, Volume 62, pages 721–726, 1977

Coherent exsolution in Fe-free pyroxenes

ROBERT H. MCCALLISTER

Department of Geosciences, Purdue University
West Lafayette, Indiana 47907

AND RICHARD A. YUND

Department of Geological Sciences, Brown University
Providence, Rhode Island 02912

Abstract

Mg-rich diopsides on the $Mg_2Si_2O_6$–$CaMgSi_2O_6$ join were synthesized from glasses or gels and subsequently annealed at atmospheric pressure between 1000° and 1350°C for varying lengths of time. A marked change in the exsolution kinetics was observed at 1325°C for $Di_{54.1}$ and at 1275°C for $Di_{63.3}$. Below these temperatures the respective compositions exsolve rapidly (in one day or less), and the resulting microstructure, observed by transmission electron microscopy, consists of closely-spaced, irregular lamellae parallel to (001). Above 1325°C (for $Di_{54.1}$) and 1275°C (for $Di_{63.3}$) no exsolution was observed after equivalent or longer annealing times. In addition, no exsolution occurred for a composition of $Di_{71.5}$ annealed at temperatures as low as 1000°C for 144 hours.

A microstructure consisting of straight widely-spaced lamellae, also parallel to (001), was observed in long-term runs of $Di_{68.4}$ annealed at 1125°C for several hundred hours; however, the method of synthesis was different from that used for the other compositions and may have introduced chemical inhomogeneities into the starting material. In all cases the exsolved phase is perfectly coherent with the host, but inverts to low pigeonite during cooling. Because of the coherency between the phases, the exsolution must occur beneath the coherent solvus, and the sharp break in the kinetics is attributed to the (001) coherent spinodal.

Introduction

During the past few years several investigators have examined the exsolution microstructure in natural pyroxenes. Nord *et al.* (1975) have recently emphasized the need for kinetic and microstructural information on pyroxenes as a basis for interpreting cooling histories of igneous and metamorphic rocks. Few studies, however, have been made on samples annealed under known conditions. McCallister (1974a and 1974b) has investigated the kinetics of exsolution in iron-free pyroxenes, and in this paper we will describe the microstructure in these and additional samples annealed below the solvus.

Exsolution lamellae in silicates may be coherent with the host, especially if the lamellar width is a few thousand A or less. The exsolved phase is said to be coherent if its lattice is continuous with the host across the lamellae interface. This coherency creates elastic strain because the compositional difference between the phases results in different lattice parameters. Minimization of this elastic strain energy determines the orientation of the coherent lamellae.

Coherent lamellae of different compositions can only be produced by exsolution, but coherency is not restricted to one mechanism. It is a necessary condition for spinodal decomposition; however, homogeneous nucleation can also produce coherent phases. The elastic strain associated with coherency has several important consequences. Inclusion of the strain energy term in the total free energy change associated with exsolution results in a reduction in temperature–composition space of the region in which coherent lamellae can form. The locus of the compositions of coexisting coherent phases defines the coherent solvus which lies within the strain-free or equilibrium solvus at all temperatures. This boundary also defines the limit of the region of homogeneous nucleation. Spinodal decomposition is limited by the coherent spinodal which is tangent to

the coherent solvus at its critical point and lies inside the coherent solvus at lower temperatures. The reader unfamiliar with these concepts can find a more detailed summary and discussion in Yund (1975a and 1975b) or more advanced discussions in Cahn (1962 and 1968) and Robin (1974a).

The coherent solvus has been identified and determined for alkali feldspars (Yund, 1974; Robin, 1974b; and Sipling and Yund, 1974 and 1976); however, similar relations have not been determined for pyroxenes. The coherent solvus may lie closer to the strain-free solvus in pyroxene systems than in the alkali feldspars because of the smaller strain energy associated with the coherency. Experimental studies have reported the identification of a coherent spinodal in the alkali feldspars (Owen and McConnell, 1974; Yund *et al.*, 1974; and Sipling and Yund, 1976), but this has not been done for pyroxenes.

Methods

The bulk compositions of all samples lie on the $Mg_2Si_2O_6$–$CaMgSi_2O_6$ join and are expressed in mole percent $CaMgSi_2O_6$(Di). Starting materials having compositions corresponding to $Di_{54.1}$, $Di_{63.3}$, and $Di_{71.5}$ were crystallized from glasses initially prepared by melting oxide mixes several times. The conditions of synthesis were 1550°C and 20 kbar in a 0.75″ piston-cylinder apparatus for 1 hour. The synthesis was carried out in Pt tubes, and W3Re–W25Re thermocouples were used to reduce the apparent temperature drift (Presnell *et al.*, 1973). The $Di_{68.4}$ was prepared by two different synthesis techniques as described by McCallister (1974a), and are referred to as Method I and Method II syntheses. Method I involved homogenization of a two-phase mixture, whereas Method II involved direct crystallization of a single-phase pyroxene from a glass, and thus more closely approximates the procedure used to prepare $Di_{54.1}$, $Di_{63.3}$, and $Di_{71.5}$. The possible way in which the exsolution results may have been affected by the synthesis procedure is discussed below.

Portions of all compositions were isothermally annealed in Pt resistance furnaces at one atmosphere and a variety of temperatures within the miscibility gap. Pt tubes were used to hold the charges, and crushed grain mounts of these samples were then examined by transmission electron microscopy using either a JEM-200A operating at 200kV or a JEM-7A at 100kV.

Results

Microstructure

In experiments using $Di_{54.1}$, $Di_{63.3}$, and $Di_{71.5}$, the exsolution microstructure, when present, consists of irregular exsolution lamellae parallel to (001), and it was observed in all properly oriented fragments. A similar lamellar structure has been referred to as a modulated exsolution microstructure by investigators who observed it in natural samples (*e.g.* Champness and Lorimer, 1971). The conditions under which this microstructure develops are shown by dots on Figure 1, and a typical example is shown in Figure 2A ($Di_{54.1}$ annealed at 1250°C for 20 hours). The open circles in Figure 1 are runs in which no microstructure was observed. The annealing times, in hours, are given in parentheses on Figure 1. For $Di_{68.4}$ prepared by Method II, no exsolution microstructure was developed at 1125°C even after annealing times in excess of 450 hours. However, material of the same composition synthesized by Method I and annealed at 1125°C for 696.5 hours developed an exsolution microstructure distinctly different from that observed in the other runs. It consisted of coarser, straight, and more continuous lamellae parallel to (001) (Fig. 2B.).

In all cases the diffraction patterns for grains in which an exsolution microstructure was observed are essentially identical. Correlation with the images indicates that the exsolution lamellae are parallel to (001) within the uncertainty of the measurement, which is about 3 degrees. The phases in both microstructures were recognized to be essentially coherent by the absence of dislocations along the interface and by the shape of certain reflections in the electron diffraction pattern. Coherency with essentially homogeneous strain within the phases requires that reflections from planes normal to the interface remain single and sharp, because the atomic planes have the same spacing in both phases, whereas atomic planes parallel (or inclined) to the lamellar interface will have different spacings depending on the compositional difference between the phases and their elastic constants. Thus, reflections from the latter may be elongated or even doubled. This fine-structure of the diffraction spots will be more complex if the lamellar spacing is a few hundred A's or less, because such a microstructure produces "side-bands" or satellite reflections about the principal Bragg reflections. These satellites are normal to the lamellae interface, and their distance from the central Bragg reflection is inversely proportional to the lamellae spacing. Thus, a microstructure such as that shown in Figure 2A produces streaking of most reflections, due to both the compositional difference of the lamellae and the periodicity of the microstructure itself (Fig. 3). The "side-bands" are not resolved when the lamellae spacing is large, and hence only the compositional difference produces observable streaking or-

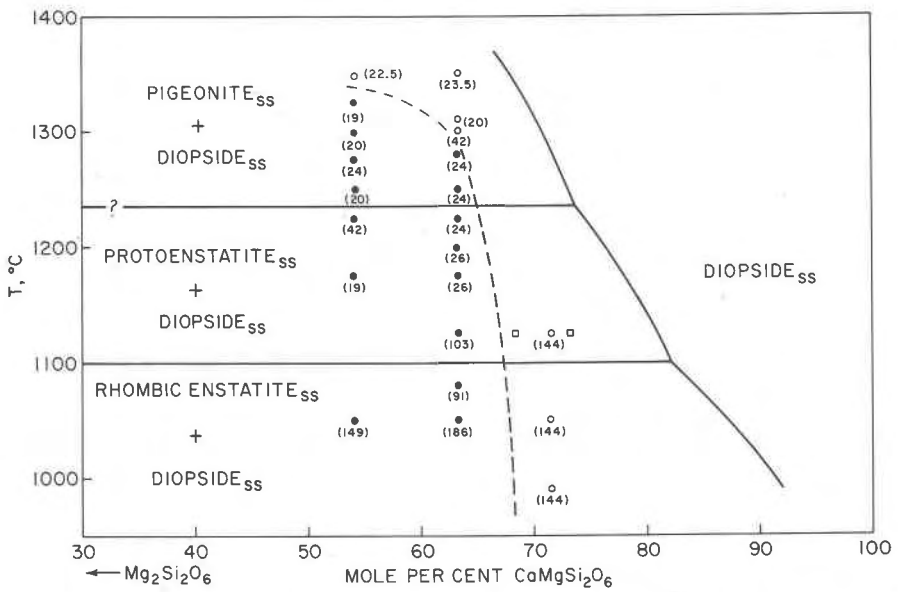

Fig. 1. Conditions of annealing experiments on the $Mg_2Si_2O_6$–$CaMgSi_2O_6$ join. Annealing times (hrs.) are shown in parentheses. Irregular lamellar microstructure observed in samples shown by solid dots and no lamellae or straight widely-spaced lamellae in samples shown by open circles and squares, respectively. The inferred position of the coherent spinodal is shown by the dashed line.

elongation around the Bragg reflections. Reflections showed no diffuseness or elongation in a direction parallel to the lamellar interface, indicating that the phases are coherent with approximately homogeneous strain.

Kinetics

The dashed curve in Figure 1 not only separates the regions within which the two distinctive microstructures are developed, but it also delineates a boundary across which the kinetics of the exsolution change markedly. For example, in experiments made with a bulk composition of $Di_{63.3}$ the modulated microstructure develops at and below 1275°C, whereas at 1300°C no exsolution is observed for this composition after approximately twice the annealing time of the 1275°C run. For the $Di_{54.1}$ bulk composition, the modulated microstructure develops at 1325°C and below after one to two days; however, in a run made with this composition at 1345°C for 22.5 hours there was no evidence of the modulated microstructure. Annealing for 144 hours at 1000° to 1125°C did not produce exsolution in $Di_{71.5}$.

Discussion and conclusions

Both microstructures observed in this study must form within the coherent solvus, because of the elastic strain associated with their coherent lamellae. The solvus shown in Figure 1 is from Kushiro (1972), and represents a revision of the original phase equilibria reported by Boyd and Schairer (1964). Because most of the lower-temperature experiments on which this solvus was based were done hydrothermally and included non-exsolution type experiments, it probably represents the strain-free solvus. However, a careful study to distinguish between the coherent and strain-free solvi in this system is needed.

The difference in exsolution kinetics as delineated by the dashed curve on Figure 1 requires explanation. We suggest that the rapid exsolution kinetics which result in the development of the modulated microstructure (Fig. 2A) indicate spinodal decomposition. The fact that the more regular microstructure (Fig. 2B) developed only after considerably longer annealing times of $Di_{68.4}$, which was initially synthesized by annealing a two-phase mixture to form a single "homogeneous" phase (Method I), suggests the possibility of coherent nucleation and growth as a mechanism. Admittedly the microstructure alone is not a sufficient criterion for determining which exsolution mechanism is operative; however, the change in kinetics across the dashed curve in Figure 1 provides additional important information. The rate of spinodal decomposition is only dependent on the interdiffusion of Ca and Mg, whereas the formation of a nucleus also requires an initial increase in the free energy of the system in order to overcome the nucleation barrier. This is consistent with the much slower rate for the formation of the regular microstructure compared with the modulated type.

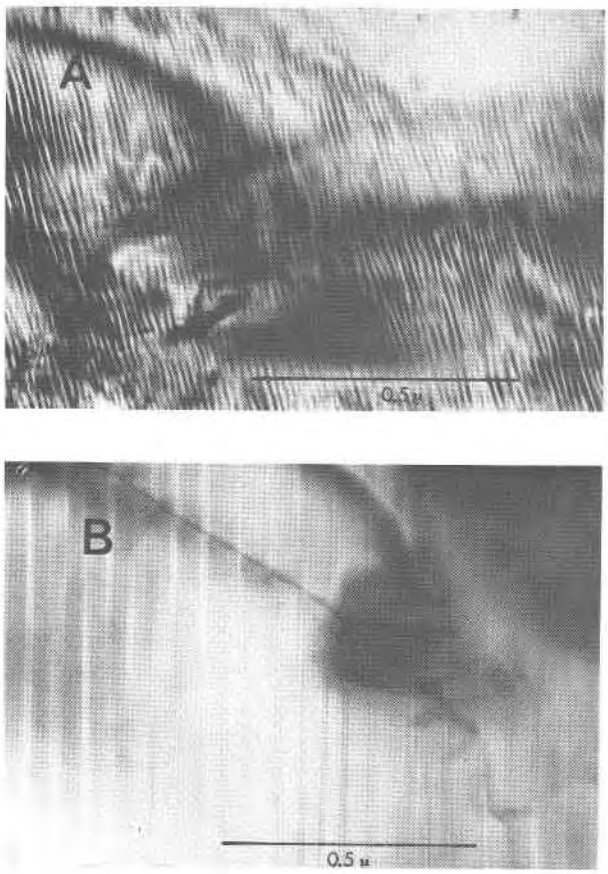

Fig. 2. Bright-field micrographs of pyroxene lamellae approximately normal to crystal fragment, and taken at 200kV. (A) Irregular lamellae in $Di_{54.1}$ annealed at 1250°C for 20 hrs. (B) Regular widely-spaced lamellae in $Di_{68.4}$ annealed at 1125°C for 696.5 hrs.

It might be argued that both microstructures form by coherent nucleation, and that the slower exsolution rate in the samples of $Di_{68.4}$ is due to a decreasing nucleation rate (larger nucleation barrier) associated with its lower supersaturation. However, this would not account for what appears to be a sharp break in the kinetics. Thus, we conclude that the most probable explanation for the change across the dashed curve on Figure 1 is a change in the exsolution mechanism, and that it represents the approximate position for the (001) coherent spinodal. It is worth noting that although the critical wavelength for spinodal decomposition increases as the coherent spinodal is approached, the relative change in the critical wavelength is rather abrupt over a narrow temperature (~10°C) or compositional (a few mole percent) interval (Cahn, 1968). Although this may cause one to underestimate the position of the coherent spinodal slightly, the error is expected to be small compared to the temperature and compositional uncertainties of the dashed line on Figure 1.

For comparison, the modulated microstructure previously described is very similar, except for orientation, to that observed in alkali feldspars. In this case its development has been attributed to spinodal decomposition (Owen and McConell, 1974 and Yund *et al.*, 1974). Champness and Lorimer (1971, 1972) have observed the fine-scale irregular lamellar microstructure in terrestrial and lunar volcanic pyroxenes and also attribute its formation to spinodal decomposition as a result of rapid cooling and the consequent high supersaturation. In addition, Nord *et al.* (1975) suggest that an augite rim in a pyroxene from lunar rock 12053 which exhibits a "tweed" exsolution microstructure and a diffraction pattern giving small $\Delta\beta$'s has exsolved spinodally. In contrast, Copley *et al.* (1974) observed a microstructure similar to Figure 2B, and suggested that it developed as a result of heterogeneous nucleation and growth in slowly cooled rocks, although, even in this case, the lamellae appear to be coherent with the host.

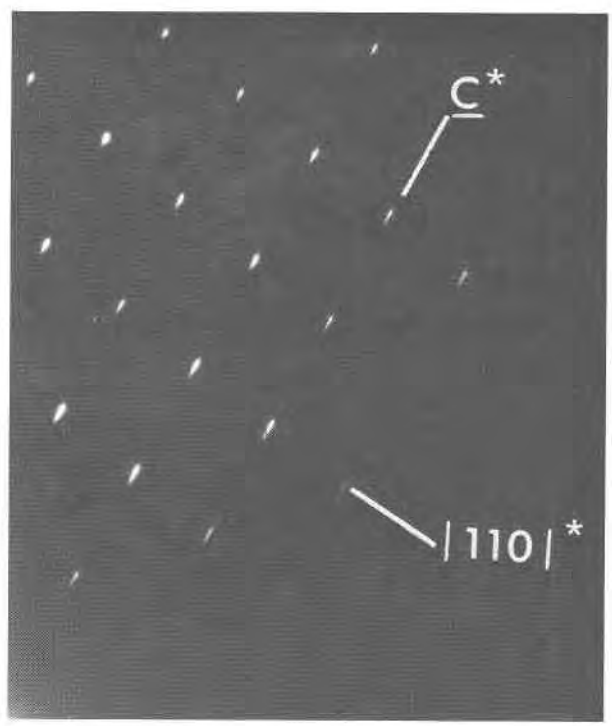

Fig. 3. Electron diffraction pattern of a crushed fragment of $Di_{54.1}$ annealed at 1175°C for 19 hrs. Elongation or streaking of reflections and the presence of satellite reflections are due to compositional differences between lamellae and the periodicity of the lamellae microstructure (see text). Lack of diffuseness or streaking of reflections except parallel to c^* indicates a high degree of coherency.

From the present study it appears that slow cooling of clinopyroxenes with low ferrosilite contents may result in coherent exsolution by nucleation and growth before the coherent spinodal is reached. Thus, it is possible that only rapidly cooled pyroxenes or those which enter the miscibility gap at low temperatures remain homogeneous until they intersect the coherent spinodal.

In order to substantiate this suggestion, a discrete clinopyroxene nodule from the Thaba Putsoa kimberlite pipe, Lesotho (supplied by F. R. Boyd) has recently been examined. This pyroxene has approximately 10 mole percent $FeSiO_3$ and a Ca/(Ca + Mg) ratio of 0.32 (this corresponds to an equilibration temperature of 1375°C when referred to the solvus of Davis and Boyd, 1966) and is believed to have been intruded at a very rapid rate. Observations made on crushed grain mounts of this material indicate that it is exsolved, and the appearance and scale of the exsolution microstructure are virtually identical to that obtained for the synthetic samples annealed for relatively short duration within the dashed curve shown on Figure 1.

In conclusion, future research should include determining the coherent spinodal surface(s) within the pyroxene quadrilateral. This is of particular importance in view of the theoretical study of Fletcher and McCallister (1974) in which it was predicted that with increasing iron content of clinopyroxenes the undercooling to the top of the (100) coherent spinodal becomes comparable to that for (001) exsolution. This may account for the observation of Nord *et al.* (1975) that both (100) and (001) compositional modulations (the "tweed" microstructure) are present in the iron-bearing lunar augite from rock 12053. Also, it will be necessary to obtain kinetic data for the different exsolution mechanisms, and to determine the coarsening kinetics of selected exsolution microstructures. Such kinetic studies can provide data needed to interpret cooling rates of natural pyroxenes.

Acknowledgments

We thank Drs. H. O. A. Meyer, J. Tullis, G. Nord, and Mr. Nabil Zaki Boctor for reviewing this manuscript. We also thank Mr. R. L. Bryant for his careful photographic work. R. H. McCallister acknowledges the support of the Geophysical Laboratory, where some of this research was done while he was a post-doctorate fellow. This work was also supported by the National Science Foundation Grant GA-21145 (RAY).

References

Boyd, F. R. and J. F. Schairer (1964) The system $MgSiO_3$–$CaMgSi_2O_6$. *J. Petrol., 5,* 275–309.

Cahn, J. W. (1962) Coherent fluctuations and nucleation in isotropic solids. *Acta Metall., 10,* 907–913.

——— (1968) Spinodal decomposition. *Trans. Metall. Soc. A.I.M.E., 242,* 166–180.

Champness, P. E. and G. W. Lorimer (1971) An electron microscope study of a lunar pyroxene. *Contrib. Mineral. Petrol., 33,* 171–183.

——— and ——— (1972) Electron microscope studies of some lunar and terrestrial pyroxenes. *Int. Mater. Symp. Berkeley Ca.,* California University Press, p. 1245–1255.

Copley, P. A., P. E. Champness and G. W. Lorimer (1974) Electron petrography of exsolution textures in an iron-rich clinopyroxene. *J. Petrol., 15,* 41–57.

Davis, B. T. C. and F. R. Boyd (1966) The join $Mg_2Si_2O_6$–$CaMgSi_2O_6$ at 30 kilobars pressure and its application to pyroxenes from kimberlites. *J. Geophys. Res., 14,* 3567–3576.

Fletcher, R. C. and R. H. McCallister (1974) Spinodal decomposition as a possible mechanism in the exsolution of clinopyroxene. *Carnegie Inst. Wash. Year Book, 73,* 369–399.

Kushiro, I. (1972) Determination of the liquidus relations in synthetic silicate systems with electron probe analysis. The system forsterite–diopside–silica at 1 atmosphere. *Am. Mineral., 57,* 1260–1271.

McCallister, R. H. (1974a) Kinetics of enstatite exsolution from supersaturated diopsides. In A. W. Hofmann, B. J. Giletti, H. S. Yoder, Jr., and R. A. Yund, Eds., *Geochemical Transport and Kinetics,* p. 152–203. Carnegie Institution of Washington, Washington, D. C.

——— (1974b) The exsolution kinetics of a diopside solid solution having the composition 54.1 mole % $CaMgSi_2O_6$, 45.9 mole % $Mg_2Si_2O_6$. *Carnegie Inst. Wash. Year Book, 73,* 392–396.

Nord, G. L., Jr., A. H. Heuer, J. S. Lally and J. M. Christie (1975) Substructures in lunar clinopyroxenes as petrologic indicators (abstr.) *Lunar Science VI,* p. 601–603. Lunar Science Institute, Houston.

Owen, D. C. and J. D. C. McConnell (1974) Spinodal unmixing in an alkali feldspar. In W. S. Mackenzie and J. Zussman, Eds., *The Feldspars, Proc. NATO Special Conf. on Feldspars, 1972,* p. 424–439. Manchester University Press, Manchester, England.

Presnell, D. C., N. L. Brenner, and T. H. O'Donnell (1973) Drift of Pt/Pt 10Rh and W3Re/W25Re thermocouples in single stage piston-cylinder apparatus. *Am. Mineral., 58,* 771–777.

Prewitt, C. T., G. E. Brown and J. J. Papike (1971) Apollo 12 clinopyroxenes: High temperature X-ray diffraction studies. *Proc. Second Lunar Sci. Conf., Geochim. Cosmochim. Acta, Supp. 2,* 59–68.

Robin, P. Y. (1974a) Thermodynamic equilibrium across a coherent interface in a stressed crystal. *Am. Mineral., 59,* 1286–1298.

——— (1974b) Stress and strain in cryptoperthite lamellae and the coherent solvus of alkali feldspars. *Am. Mineral., 59,* 1299–1318.

Sipling, P. J. and R. A. Yund (1974) The coherent solvus for the sanidine–analbite series (abstr.) *Geol. Soc. Am. Abstr. and Programs, 6,* 958.

——— and ——— (1976) Experimental determination of the coherent solvus for sanidine–high albite. *Am. Mineral., 61,* 897–906.

Yund, R. A. (1974) Coherent exsolution in the alkali feldspars. In A. W. Hofmann, B. J. Giletti, H. S. Yoder, Jr., and R. A. Yund, Eds., *Geochemical Transport and Kinetics,* p. 171–183. Carnegie Institution of Washington, Washington, D. C.

——— (1975a) Subsolidus phase relations in the alkali feldspars

with emphasis on coherent phases. In P. H. Ribbe, Ed. *Feldspar Mineralogy,* p. Y1–28. Mineral. Soc. Am. Short Course Notes Vol. 2.

——— (1975b) Microstructure, kinetics, and mechanisms of alkali feldspar exsolution. In P. H. Ribbe, Ed. *Feldspar Mineralogy,* p. Y29–57. Mineral. Soc. Am. Short Course Notes Vol. 2.

———, A. C. McLaren and B. E. Hobbs (1974) Coarsening kinetics of the exsolution microstructure in alkali feldspar. *Contrib. Mineral. Petrol., 48,* 45–55.

Manuscript received, January 2, 1976; accepted for publication, January 5, 1977.